

# Search for extra dimensions with the ATLAS detector



LPCC Exotica 12.04.2011 – on behalf of the ATLAS Collaboration/Exotics group  
Helenka Przysiezniak LAPP/CNRS

# Why extra dimensions?

Somehow could be an elegant way out of the hierarchy problem

$$M_{\text{weak}} \rightarrow M_{\text{planck}}$$

Still many think that the hierarchy problem is just swept under the carpet  
i.e. masses are well behaved but why so many extra dimensions? or why so small?

Anyhow

ATLAS has investigated two rather theoretically elegant models

**Small extra d's**

**à la Randall Sundrum**

where  $M_{\text{Planck}}^{\text{Eff}} \approx M_{\text{weak}}$

thanks to a warped geometry :

“let's just add an exponential somewhere in there”  
only need one extra dimension

**Small extra d's**

**à la Universal Extra Dimension**

with a few large ones  
mocking SUSY along the way



# Randall Sundrum graviton resonance

Universe has two 4-d surfaces bounding slice of 5-d spacetime  
SM fields live on TeV brane

Gravity lives everywhere i.e. on TeV and Planck branes and in bulk

Exponentially warped fifth dimension

$$ds^2 = e^{-2kr_c|y|} \eta_{\mu\nu} dx_\mu dx_\nu - r_c^2 dy^2$$

where  $k$  curvature, of order of Planck scale

$r_c$  compactification radius

$$\Lambda_\pi = \bar{M}_{\text{Pl}} \exp(-k\pi r_c)$$

where  $M_{\text{Pl}}$  is Planck scale /  $\sqrt{(8\pi)}$  and  $kr_c \sim 10-12$

KK excitations of spin 2 graviton with mass splitting  $\sim$  TeV

Dimensionless coupling  $k/M_{\text{Pl}}$  to SM fields

$k/M_{\text{Pl}} \approx 0.01-1.0$  considered in theoretical calculations

but 0.01-0.1 favoured values

**Resonance  $G \rightarrow$  SM particle pairs : diphotons in ATLAS study**

Value of $k/\bar{M}_{\text{Pl}}$	95% CL Mass Limit (GeV)	
	D0 Expt	CDF Expt
0.01	560	472
0.10	1050	976

Diphotons + dileptons

# G → $\gamma\gamma$ cross sections X BR

Graviton mass (GeV)	Value of $k/\bar{M}_{Pl}$	Graviton width (GeV)	LO $\sigma \times BR$ (fb)
300	0.01	0.045	1052
500	0.01 *	0.075	82.5
	0.03	0.680	741.8
700	0.01	0.089	12.98
	0.03	0.871	116.3
	0.05	2.646	329.5
800	0.01 *	0.120	6.0
	0.03	1.088	54.4
	0.05	2.79	150.1
	0.10	12.09	600.9
900	0.03	1.15	26.94
	0.05	2.98	74.99
	0.07	5.67	142.8
	0.10	12.06	293.1
1000	0.01 *	0.151	1.56
	0.03	1.361	13.9
	0.05	3.780	39
	0.10	15.12	152.6
1100	0.05	3.75	20.99
	0.07	7.44	41.15
	0.10	14.93	83.46
	0.20	57.6	326.5
1250	0.05	4.725	9.08
	0.07	8.23	17.96
	0.10	18.90	36.1
	0.15	37.3	81.07
	0.20	65.2	142.2

# Data sample – 36 pb<sup>-1</sup> – event selection

- Good Run List
- Trigger diphoton with  $ET > 15$  GeV
- Primary Vertex with at least 3 good tracks
- $\geq 2$  photons
- $|\eta_{S2}| < 1.37$  or  $1.52 < |\eta_{S2}| < 2.37$   
( Electromagnetic (EM) +  
Internal detector  
excluding EM barrel/endcap crack)
- $ET_{ph1,2} > 25$  GeV
- loose photon selection  
(rectangular cuts on shower shaper variables)

**8090 events selected**

**1650 events with  $m_{\gamma\gamma} > 120$  GeV**

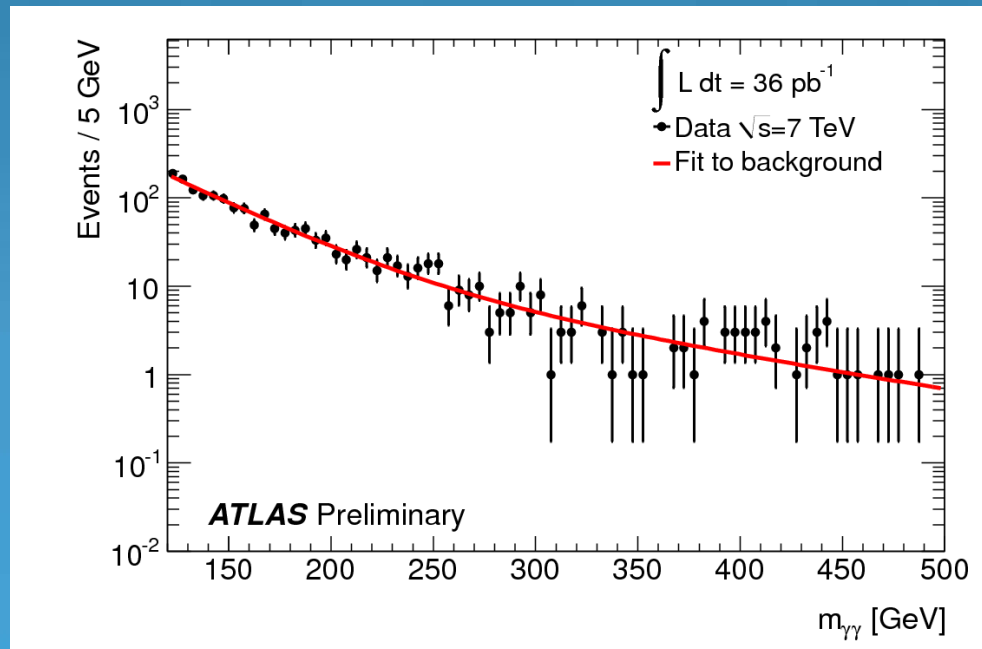


# Main backgrounds

- SM diphoton production (irreducible)
- QCD + jet and multijet events with at least one fake photon (reducible)

inclusive shape of background  $m_{\gamma\gamma}$  distribution determined from fit to  $120 \text{ GeV} < m_{\gamma\gamma} < 500 \text{ GeV}$  control region (region excluded by Tevatron for  $k/M_{\text{Pl}} < 0.1$ )

When setting a limit for a 500 GeV graviton background fit restricted to  $120 \text{ GeV} < m_{\gamma\gamma} < 430 \text{ GeV}$  range



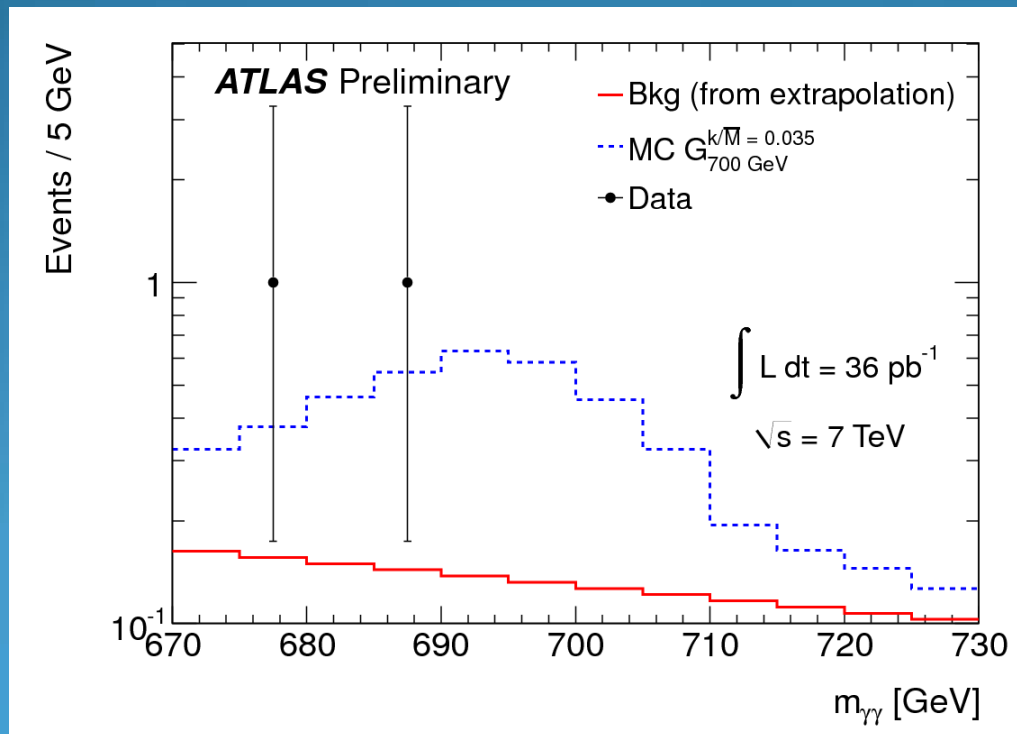
Diphoton candidate  $m_{\gamma\gamma}$  distribution in control region. Superimposed is the result of a fit to the data of the background parametrization of the sum of two exponential functions. 94% CL

# Comparison to MC signal templates

Observed invariant mass distribution within a window around test mass compared with histograms of expected signal and background templates.

Background prediction determined by extrapolating background fit function into search region of higher diphoton masses.

Signal templates determined from fully simulated signal MC samples



Expected signal (dashed) extrapolated background (solid), and observed (points) distributions in a  $\pm 30$  GeV mass window around  $m_G = 700 \text{ GeV}$   $k/M_{Pl} = 0.035$ .

# Systematic uncertainties

<b>Source</b>	<b>Signal (%)</b>
Luminosity	3.4
Signal MC statistics	1
Trigger	1
Photon reco+id	3.8
Pileup	3.6
Photon quality	0.5
Correct bunchXing	2.0
Photon energy resolution/scale (shape)	
PDF	5.2-9.2
Factorization and renormalization scales	6.0

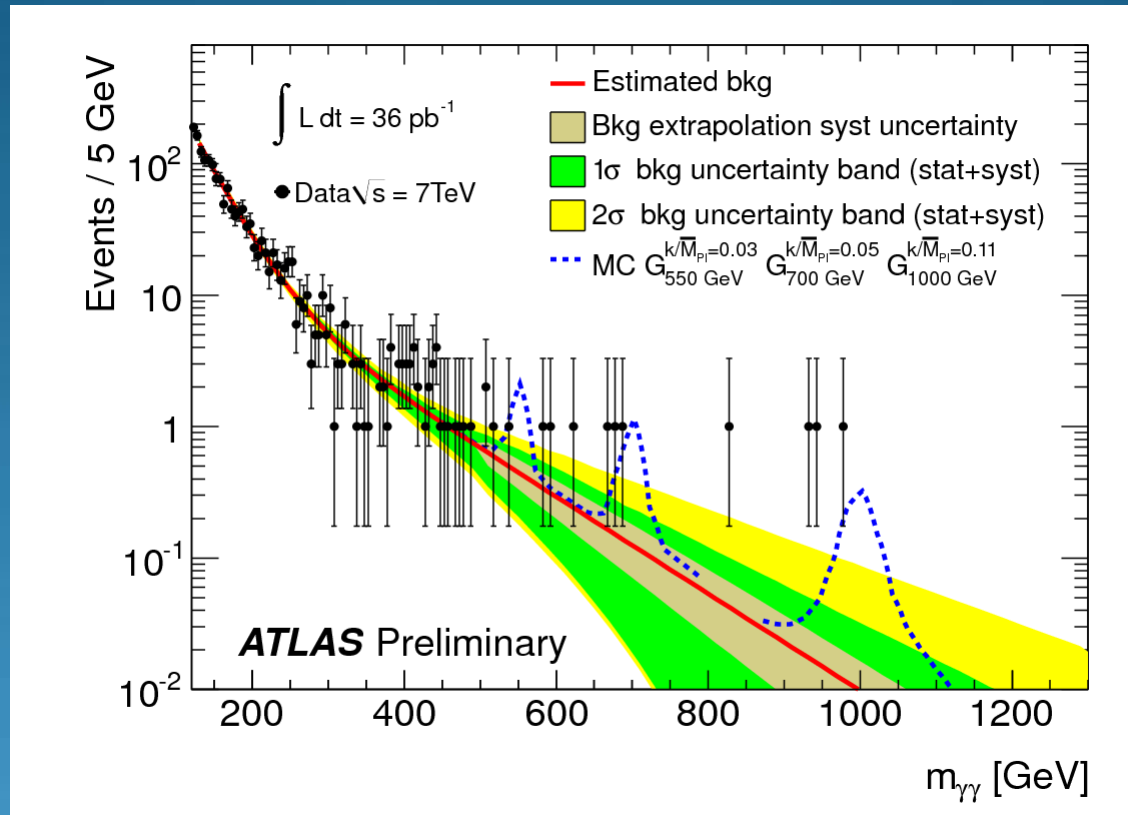
## **Background systematic uncertainties**

Fit range (brown band)

Statistical and systematic fluctuations (green/yellow bands)

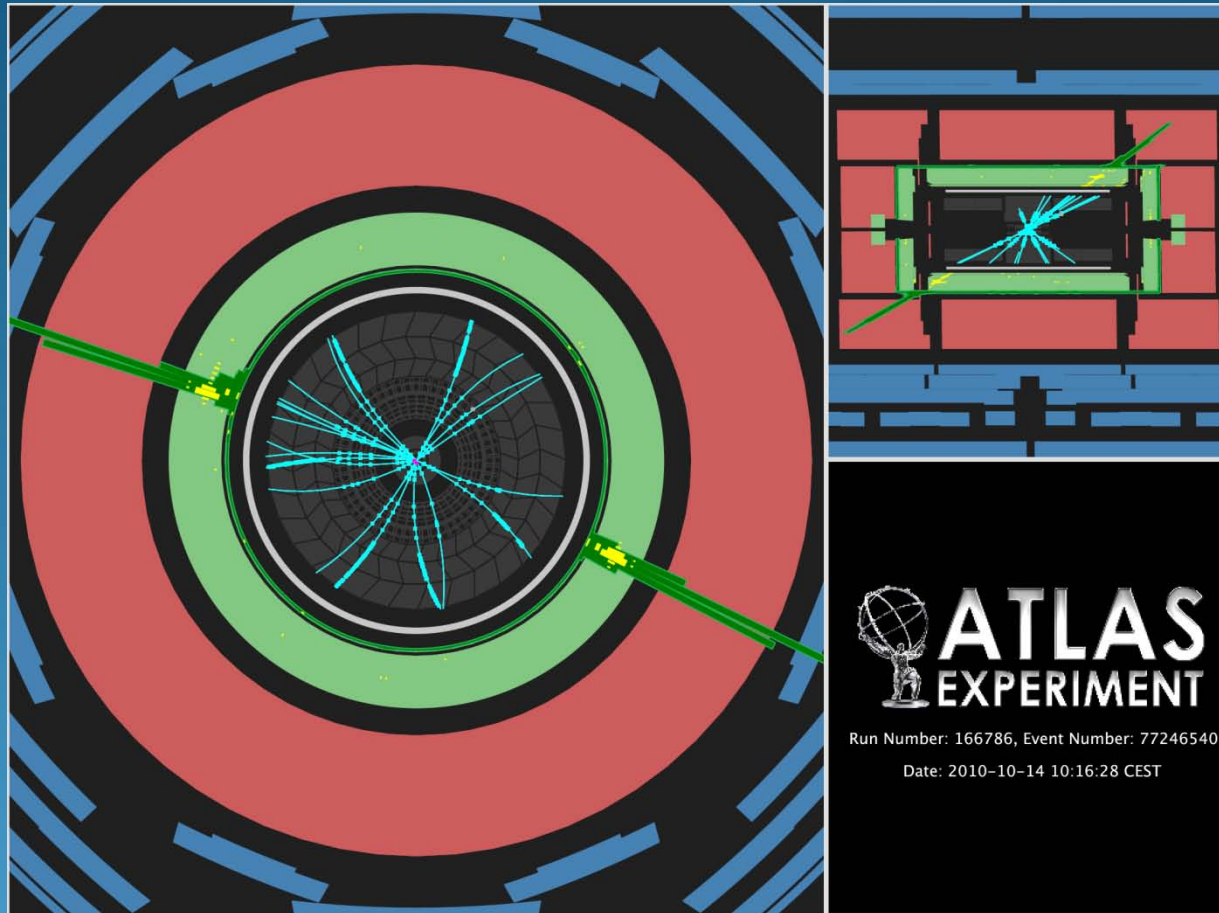


# Results



Reconstructed  $m_{\gamma\gamma}$  distribution for data (points) and expected background (red line). Also shown are graviton signals of masses 550, 700 and 1000 GeV and couplings  $k/\overline{M}_{\text{Pl}} = 0.03, 0.05$  and  $0.11$ , respectively. Signal normalized to number of expected events for  $36 \text{ pb}^{-1}$ .

# Highest $m_{\gamma\gamma}$ event passing tighter photon selection



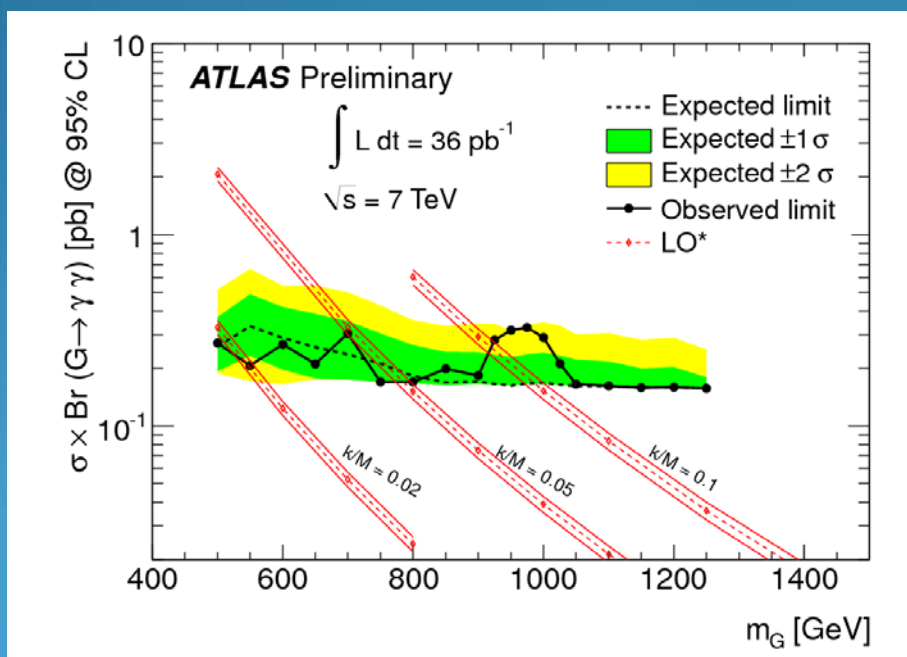
An event display of the highest invariant mass diphoton event in which both candidate photons satisfy the more stringent photon identification cuts. The highest transverse momentum photon has  $p_T = 194$  GeV and  $(\eta, \phi) = (-1.32, -0.44)$ . The trailing photon has  $p_T = 173$  GeV and  $(\eta, \phi) = (1.10, 2.82)$ . The diphoton invariant mass is equal to 679 GeV.

# Extraction of limit

Modified frequentist method [A.L. Read, J. Phys. G **28**, 2963 (2002).]

Performing pseudo-experiments to calculate CLs+b and CLb for CLs = CLs+b/CLb  
CLs as a function of a cross-section scaling factor  $\mu$  obtained keeping the mass window fixed.  
A scan is performed over a range of  $\mu$  until one crosses the CLs = 0.05 value  $\rightarrow$  upper limit

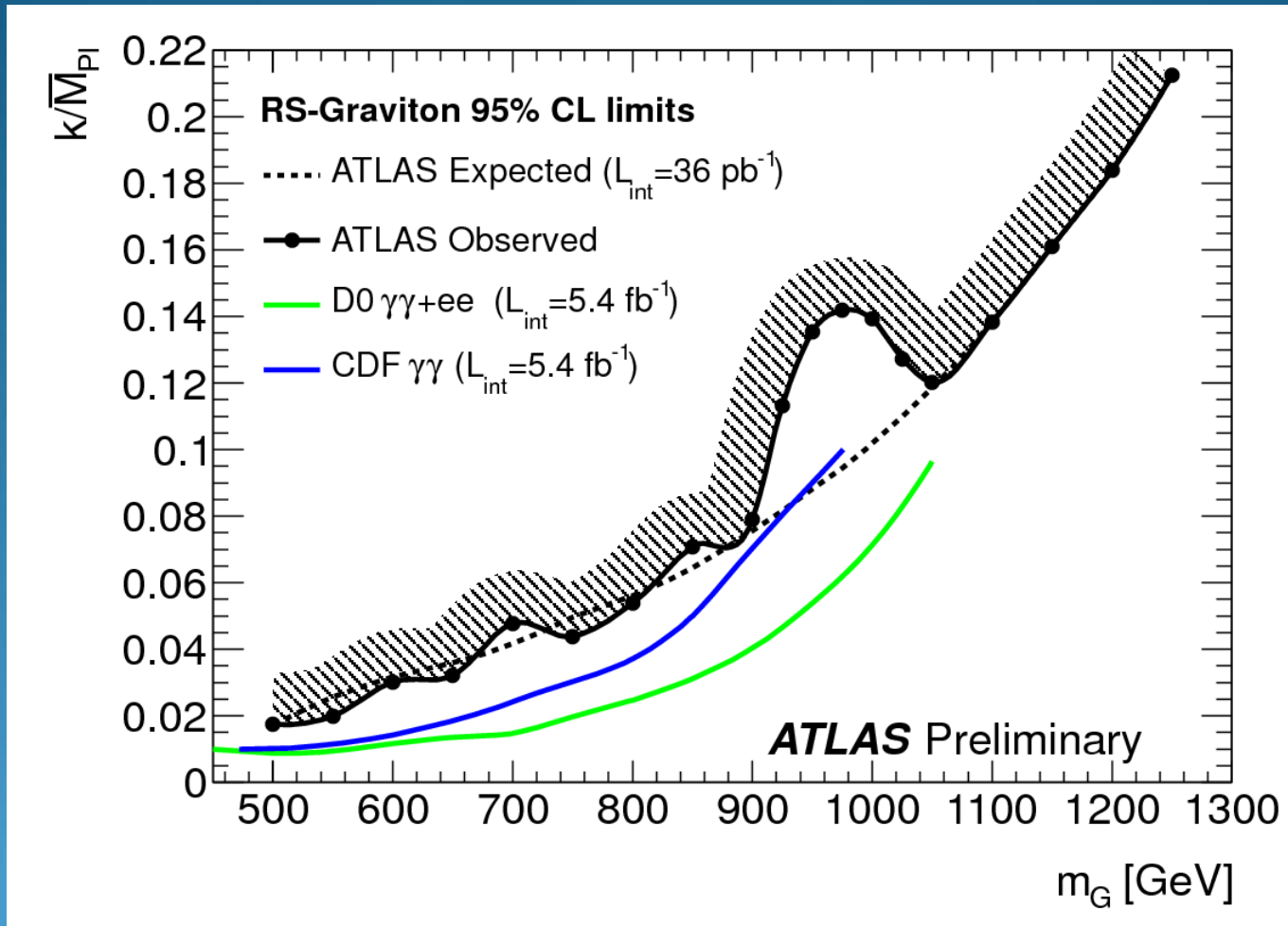
For a given mass, re-scaling of cross-section implies change in width of resonance.  
At each mass point, use available signal template with  $k/M_{Pl}$  value closest to expected limit  
 $\rightarrow$  change in the shape is minimized



95% CL on the production Xsection X BR  
of RS graviton  $\rightarrow \gamma \gamma$   
as a function of  $m_G$   
Superimposed are  
theoretical Xsection prediction bands  
for a variety of  $k/M_{Pl}$  values.

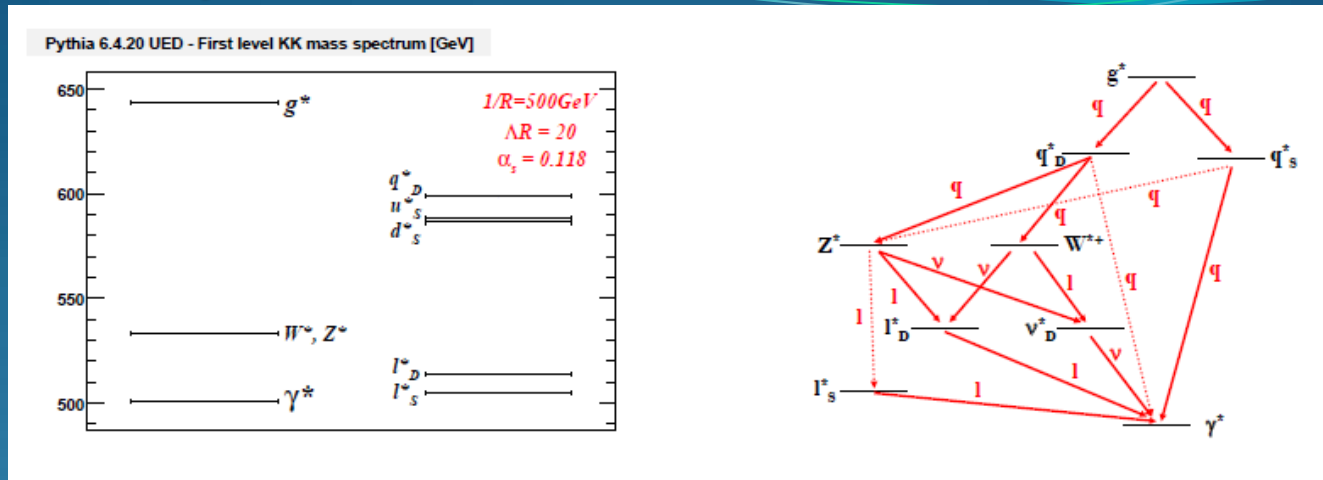
**Exclude at 95% CL RS graviton  
masses  $\leq 545$  (920) GeV  
for  $k/M_{Pl} = 0.02$  (0.1)**

# Extraction of limit



95% CL excluded region in the plane of  $k/M_{\text{Pl}}$  versus graviton mass.  
Also shown are the expected limit and published limits from the Tevatron experiments.

# Gravity mediated one Universal Extra Dimension



“Universal” == ALL SM particles propagate into the XtraD ( $\delta = 1$ ;  $1/R \sim 1\text{TeV}$ )  
 $n=1,2,3,\dots$  Kaluza Klein (KK) excitations for each SM particle ( $n=0$ )  
 $R$  : compactification scale

Mass degeneracy  $m_n^2 = n^2/R^2 + m_{SM}^2$  lifted by radiative corrections  
 $\Lambda$  : cutoff scale for radiative corrections

→ quark and gluon KK excitations cascade decay down to Lightest KK Particle  $\gamma^*$

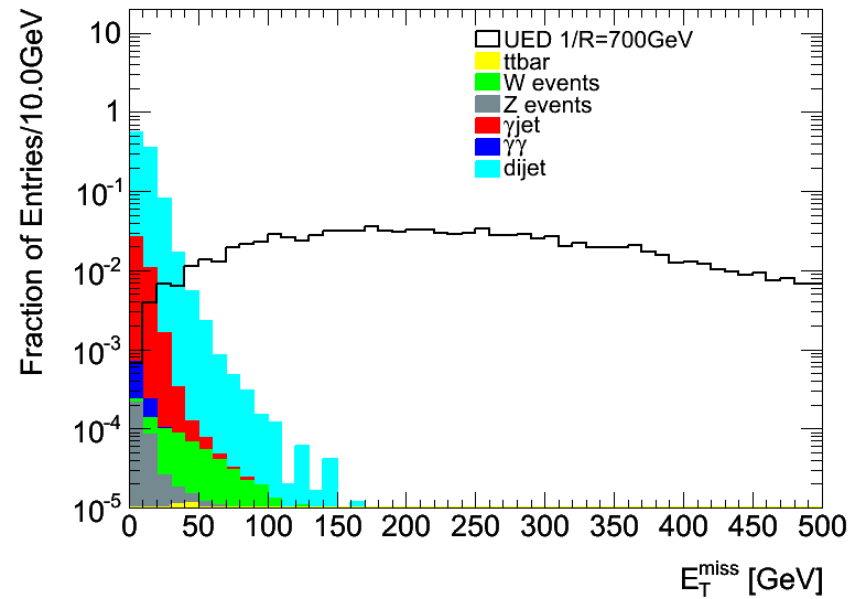
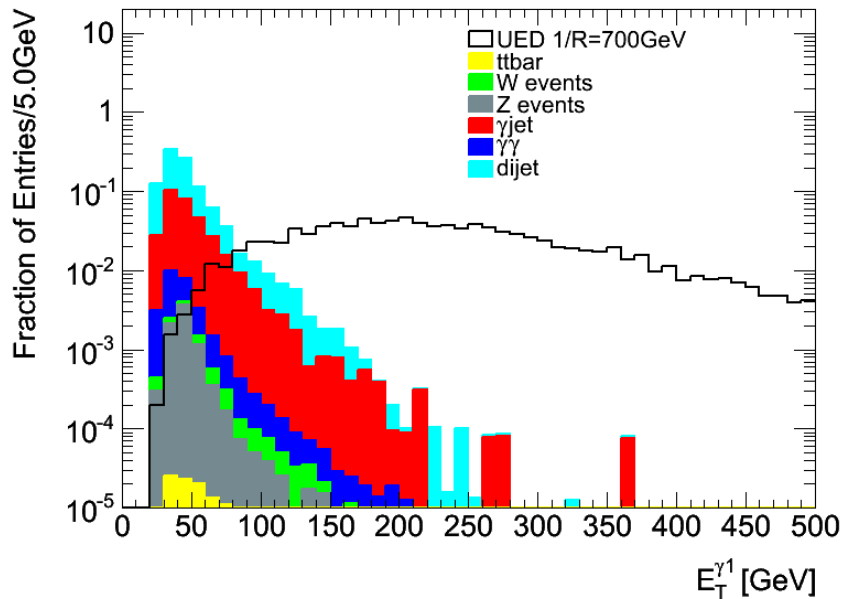
If the “thick brane”, where the SM particles propagate,  
 is embedded in a larger space of  $(4+N)$ -dim (of size<sup>-1</sup>  $\sim eV$ ) where only gravitons propagate  
 → gravity mediated decays become possible and graviton acquires mass between 0 and  $1/R$   
 Two KK partons cascade decay to give  $2 \times (\gamma^* \rightarrow \gamma + \text{Graviton})$

**High pT diphoton + MET**

**D0@Tevatron exclude  $1/R < 477\text{ GeV}$**

# Xsections – 3.1 pb-1 data sample - event properties

Signal 1/R [GeV]	Xsection [pb]	# Events for 3.1 pb-1
300	709.6	604
600	8.599	12.1
700	2.770	4.21
800	0.966	1.51
900	0.354	0.58
1000	0.132	0.22



# Event selection

## Baseline cuts



- Good Run List
- Trigger single EM object  $ET > 20$  GeV
- PV with at least 3 good tracks and  $|PVz| < 150$  mm
- Jet cleaning
- $\geq 2$  photons
- $|\eta_{S2}| < 1.37$  or  $1.52 < |\eta_{S2}| < 1.81$   
(barrel+endcap presampler EM region  
excluding barrel/endcap crack)
- $ET_{ph1,2} > 25$  GeV

## Signal selection cuts

- Isolation cone  $ET(\eta \times \phi = 0.2)_{ph1,2} < 35$  GeV
- loose photon selection  
(rectangular cuts on shower shaper variable)
- $MET > 75$  GeV  
(all calorimeter cell clusters but no muons)

Signal efficiencies range from  $\sim 25\%$  to  $\sim 50\%$

# Data driven background estimation

Limited MC statistics (dijets) make it impossible to determine background accurately  
Observed big differences between MC and data QCD multi-jets production

→ Measure MET distribution from data and extrapolate to the high MET signal region

In data, events with

→ 1. fake MET

→ 2. genuine MET with fake photons

→ 3. irreducible genuine MET with true photons  
(neglected due to fb-sized cross-sections)



# Data driven background estimation

## 1. Fake MET events

Caused by MET mis-measurements, MET resolution effects, originating from  $\gamma\gamma$  -  $\gamma$ jet – QCD multi-jets

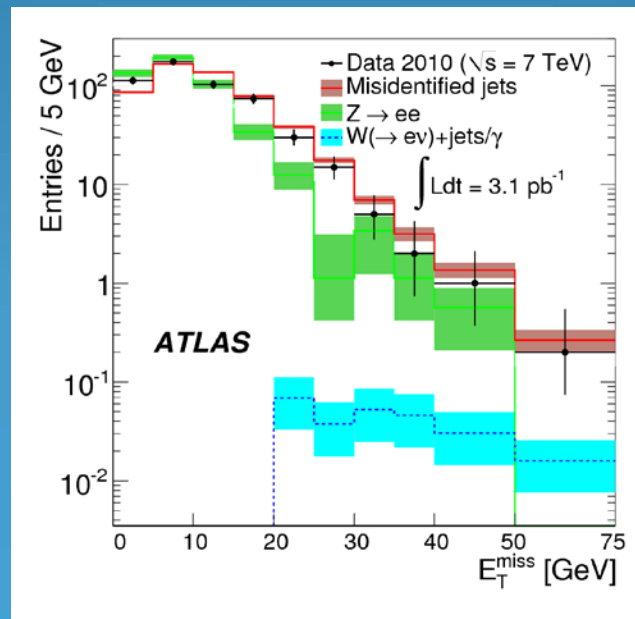
→ Identify  $Z \rightarrow ee$  :

same kind of behavior as  $\gamma\gamma$

→ Identify anti-signal-selection control sample

i.e. at least 1 of 2 most energetic photons is anti-loose :  
mostly  $\gamma$ jet – QCD multi-jets

Fit both contributions to data low MET region ( $\text{MET} < 20 \text{ GeV}$ )



# Data driven background estimation

## 2. Genuine MET but fake photons

Neutrino + one or two fake photons e.g.

W (with or without  $\rightarrow e\nu$ ) + jets (includes  $T\bar{T}$ , diboson production, etc.)

$W \rightarrow e\nu$  + gamma (small)

Dominant contribution is from  $W \rightarrow e\nu + X$  (motivated by MC studies)  
where electron mis-identified as photon and second photon is mostly jet faking

$\rightarrow$  Identify  $W \rightarrow e\nu$  events under  $W M_T$  peak  
and then require there also be a loose photon with  $E_T > 25$  GeV :  $N_{\text{evts}}$

$\rightarrow$  Determine fake rate of electron faking photon  
using  $Z \rightarrow ee$  events + tag-and-probe technique :

Identify events with tight tag and tight probe di-electrons under Z peak  $\rightarrow N_1$   
Identify events with tight tag electron and one loose photon under Z peak  $\rightarrow N_2$

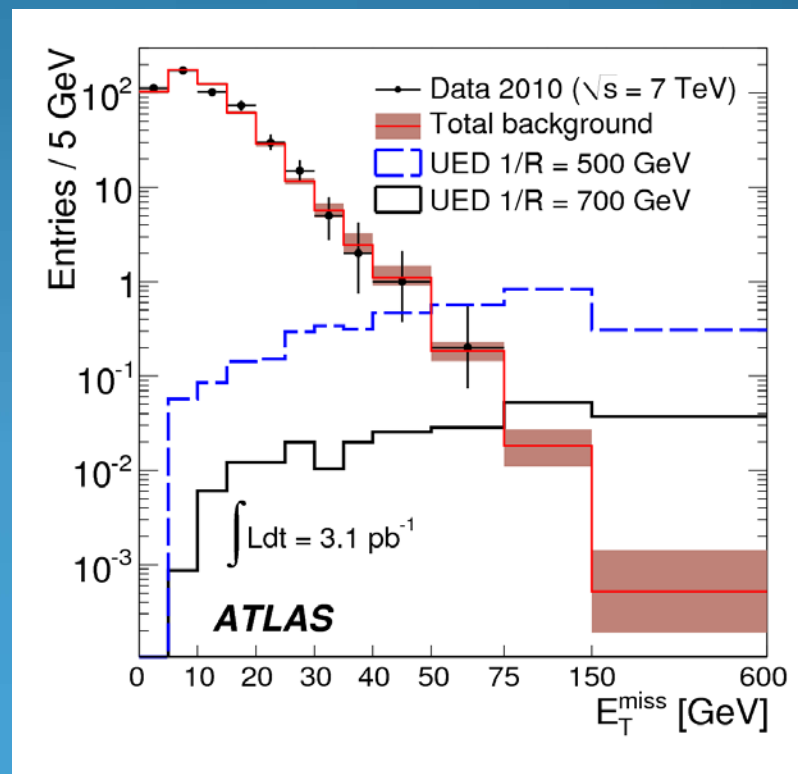
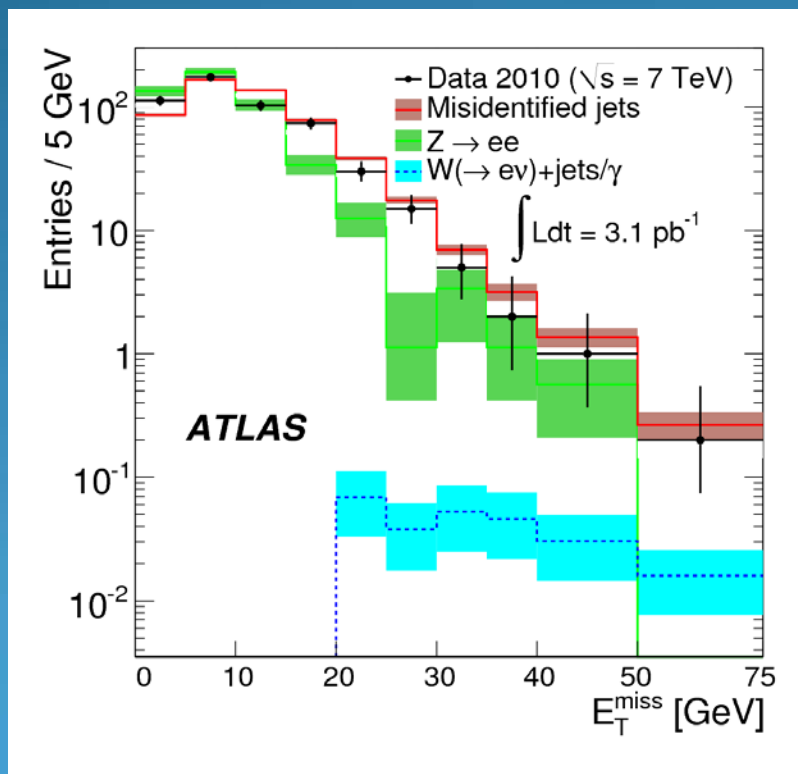
$\rightarrow$  Fake rate =  $N_2 / N_1$

Overall number of W events expected for  $3.1 \text{ pb}^{-1} = N_{\text{evts}} \times N_2 / N_1$

# Data driven background estimation

MET<20 GeV region background distribution, determined by normalizing the weighed Zee + anti-signal control sample (fake MET) to the data passing all signal selection cuts, is extrapolated to the MET>20 GeV while adding the W+X (genuine MET) contribution

**For MET>75 GeV  $\rightarrow N_{\text{bgd}} = 0.32 \pm 0.16$  (stat)**



# Systematic uncertainties

Source	Signal (%)
Luminosity	11
Photon reco+id	4
Pileup	2
MET	1
Signal MC statistics	1
-----	
Total	12
Theoretical (PDF)	8

## Background systematic uncertainties

varying within its error fraction determined in fit of QCD background,  
varying definition of misidentified jet sample,  
eliminating photon isolation cut

$$N_{\text{bgd}} = 0.32 \pm 0.16 (\text{stat}) + 0.37 / -0.10 (\text{syst})$$

# Result and statistical interpretation

Zero data events observed

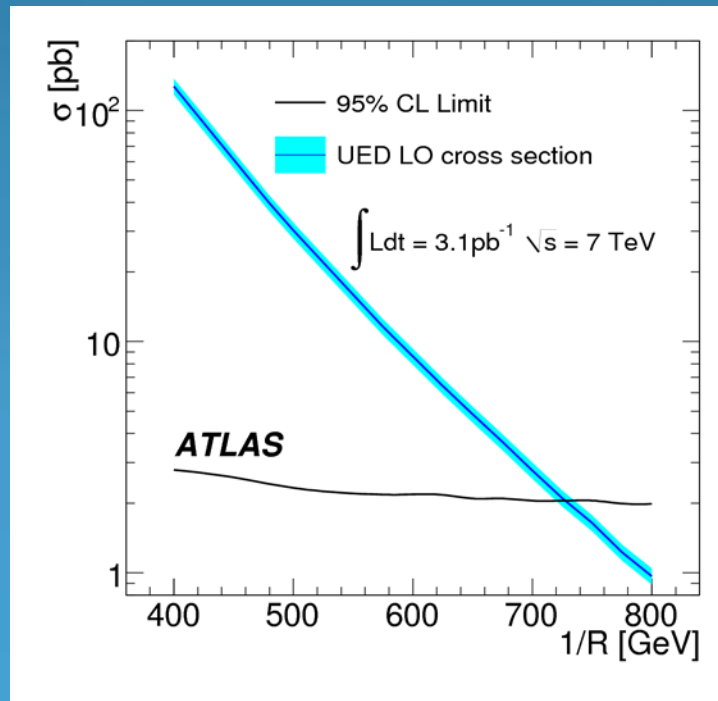
12% signal acceptance systematic uncertainty

8% PDF uncertainty

$0.32 \pm 0.16$  (stat)  $+0.37/-0.10$  (syst) background estimated from data

Using Bayesian method with Gaussian prior (also tested LogNormal/Uniform/D0/CDF)  
exclude @ 95% CL gravity mediated one UED with

**$1/R \leq 728$  GeV and  $\Lambda R = 20, N = 6, M_D = 5$  TeV**



95% CL upper limits  
on UED prod. Xsection  
+LO theory Xsection prediction,  
as a function of  $1/R$ .  
Shaded band is pdf uncertainty.

## Conclusion/outlook/ongoing thoughts



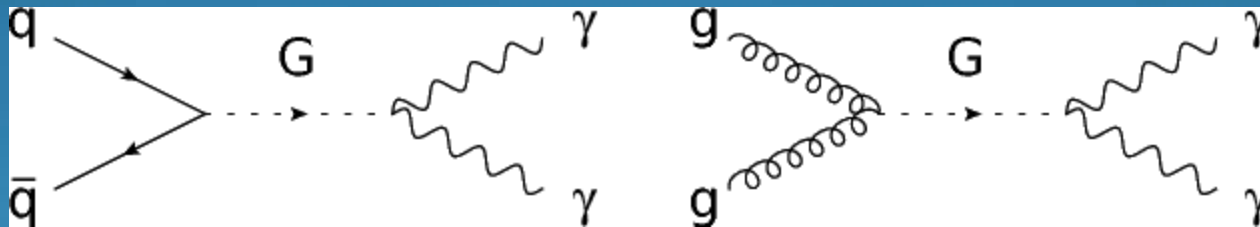
"Matthews ... we're getting another one of those strange 'aw blah es spon yol' sounds."

Looking into 2011 data  
Running over full 2010 data set for UED

Looking at a generalized UED model  
where masses are set free

# Backup





Leading order Feynman diagrams depicting RS graviton production at a hadron collider, followed by the decay  $G \rightarrow gg$ .



# Randall Sundrum graviton resonance xsections

Graviton mass (GeV)	Value of $k/\bar{M}_{Pl}$	Graviton width (GeV)	LO $\sigma \times BR$ (fb)
300	0.01	0.045	1052
500	0.01 *	0.075	82.5
	0.03	0.680	741.8
700	0.01	0.089	12.98
	0.03	0.871	116.3
	0.05	2.646	329.5
800	0.01 *	0.120	6.0
	0.03	1.088	54.4
	0.05	2.79	150.1
	0.10	12.09	600.9
900	0.03	1.15	26.94
	0.05	2.98	74.99
	0.07	5.67	142.8
	0.10	12.06	293.1
1000	0.01 *	0.151	1.56
	0.03	1.361	13.9
	0.05	3.780	39
	0.10	15.12	152.6
1100	0.05	3.75	20.99
	0.07	7.44	41.15
	0.10	14.93	83.46
	0.20	57.6	326.5
1250	0.05	4.725	9.08
	0.07	8.23	17.96
	0.10	18.90	36.1
	0.15	37.3	81.07
	0.20	65.2	142.2

G Mass [GeV]	$k/\overline{M}_{\text{Pl}}$	Mass Window [GeV]	$N_{\text{Exp}}^S$	$N_{\text{Exp}}^B$	$N_{\text{Obs}}$
500	0.03	$\pm 15$	$12.8 \pm 2.1$	$2.24 \pm 0.55$	3
550	0.03	$\pm 30$	$7.9 \pm 1.3$	$5.5 \pm 2.3$	1
600	0.025	$\pm 30$	$3.4 \pm 0.6$	$3.6 \pm 2.2$	3
650	0.04	$\pm 30$	$5.5 \pm 0.9$	$2.4 \pm 1.7$	3
700	0.035	$\pm 30$	$2.8 \pm 0.5$	$1.6 \pm 1.3$	2
750	0.05	$\pm 35$	$3.9 \pm 0.6$	$1.2^{+1.2}_{-1.1}$	0
800	0.05	$\pm 35$	$2.6 \pm 0.4$	$0.80^{+0.98}_{-0.75}$	1
850	0.06	$\pm 40$	$2.7 \pm 0.4$	$0.60^{+0.83}_{-0.60}$	1
900	0.08	$\pm 50$	$3.4 \pm 0.6$	$0.50^{+0.84}_{-0.50}$	2
925	0.085	$\pm 55$	$3.3 \pm 0.5$	$0.45^{+0.79}_{-0.44}$	3
950	0.09	$\pm 60$	$3.1 \pm 0.5$	$0.40^{+0.75}_{-0.40}$	3
975	0.11	$\pm 70$	$4.0 \pm 0.6$	$0.38^{+0.81}_{-0.38}$	3
1000	0.13	$\pm 90$	$4.8 \pm 0.8$	$0.42^{+0.92}_{-0.41}$	3
1025	0.13	$\pm 90$	$4.1 \pm 0.7$	$0.34^{+0.79}_{-0.33}$	2
1050	0.13	$\pm 90$	$3.6 \pm 0.6$	$0.27^{+0.68}_{-0.27}$	1
1100	0.15	$\pm 110$	$3.5 \pm 0.6$	$0.23^{+0.67}_{-0.23}$	0
1150	0.15	$\pm 115$	$2.6 \pm 0.4$	$0.16^{+0.52}_{-0.16}$	0
1200	0.2	$\pm 165$	$3.5 \pm 0.6$	$0.18^{+0.66}_{-0.17}$	0
1250	0.2	$\pm 165$	$2.7 \pm 0.4$	$0.11^{+0.46}_{-0.11}$	0

Table 2: Mass windows chosen to compute the  $\text{CL}_s$  for each predicted graviton signal of a given mass and  $k/\overline{M}_{\text{Pl}}$  value. The expected number of signal ( $N_{\text{Exp}}^S$ ) and background ( $N_{\text{Exp}}^B$ ) events within the mass window are also shown, together with the number of observed data events ( $N_{\text{Obs}}$ ). The errors shown are quadrature sums of the statistical and systematic uncertainties.

One example of such templates for a 700 GeV graviton with  $k/\text{MPI} = 0.035$  is shown in Fig. 3.

Each bin of the histograms is treated as a separate counting channel.

Systematic uncertainties are included as nuisance parameters on the expected number of events with Gaussian distributions [11].

A given systematic uncertainty is taken as fully correlated across all bins of a histogram.

The various systematic uncertainties are assumed to be uncorrelated with each other.

For each graviton mass, a different mass window was chosen for the search, in order to contain at least 90% of the signal in the window, including both the dependence of the resonance natural width on the value of  $k/\text{MPI}$  and the ET dependence of the detector resolution.

The chosen mass windows are given in Table 2, together with the expected number of signal and background events and the observed number of candidates.

In order to study the systematic uncertainty attributed to the background tails which might not be correctly described by the extrapolation function, the background parametrization was fit to data in different ranges of the diphoton invariant mass.

For a given test mass the fit was performed up to 100 GeV away from the test mass in steps of 100 GeV.

The largest difference in the expected number of events from these various fits and the nominal fit up to 500 GeV was taken as the systematic uncertainty of the fit extrapolation and added in quadrature to the statistical uncertainty.

The result of the background extrapolation uncertainty as a function of diphoton candidate invariant mass is shown as the brown band on Fig. 4.

The statistical uncertainty on the background shape extrapolation was determined by considering the statistical uncertainty on the background fit parametrization.

To determine this effect, pseudoexperiments were performed by varying each bin in the control region according to a Poisson distribution around the measured value, refitting the so-obtained pseudo-data sample, and determining the fluctuation of the expected number of background events within the fit window.

The  $\pm 1(2)$  standard deviation bands were then determined by taking the integral of the spread of background around the nominal value such that 68% (95%) of events were contained within the range.

The statistical and systematic uncertainties determined are represented by green and yellow bands on Fig. 4.

The MRST2007lomod parton distribution function (PDF) set [13] has been used to determine the cross section of the graviton signals with PYTHIA.

In order to estimate the systematic uncertainties due to the choice of PDF, the MSTW2008lo90cl PDF [14] set was used to change the value of the 20 eigenvalues by  $\pm 1$  sigma.

The uncertainty coming from the PDF was estimated using the difference given by the modified PDF sets and the central value.

The systematic uncertainty increases with the mass of the graviton. The uncertainty varies from 5.2–9.2% for masses between 500–1250 GeV.

The systematic uncertainty due to the factorization and renormalization scales was estimated by changing the scale from the nominal value of 1 to 0.5 and 2. This modification has at most a 6% effect on the graviton signal cross section.

Modified frequentist method [A.L. Read, J. Phys. G **28**, **2963 (2002).**]  
used to determine limit by performing pseudo-experiments  
to calculate  $CL_{s+b} = P(LLR \geq LLR_{obs} | s + b)$  and  $CL_b = P(LLR \geq LLR_{obs} | b)$ ,  
with  $P$  representing the conditional probabilities.

$CL_s$  is then defined as  $CL_s = CL_{s+b}/CL_b$ .

By repeating implementations of the fit procedure for each mass point,  
the  $CL$  in the signal ( $CL_s$ ) as a function of a cross-section scaling factor  $\mu$   
was obtained keeping the mass window fixed.

A scan is performed over a range of  $\mu$  until one crosses the  $CL_s = 0.05$  value.

The scaling factor  $\mu$  for a 95%  $CL$  exclusion was calculated by a linear interpolation  
between these points and then converted into an upper limit.

For a given mass,

a re-scaling of the cross-section would imply a change in the width of the resonance.

Thus, for each mass point,

the available signal template with the  $k/MPI$  value closest to the expected 95% limit was chosen.

This way, the change in the shape was minimized.

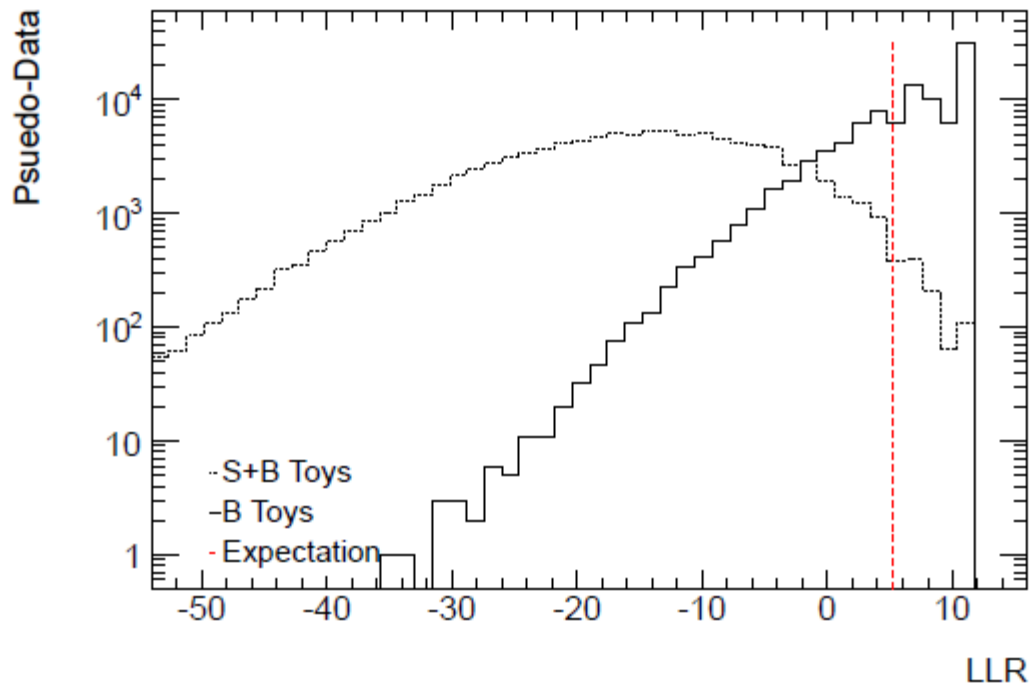


Figure 22: LLR distributions for generated signal+ background (dashed) and background-only (solid) pseudo-data. The dashed vertical line represented the expected value for the null hypothesis.



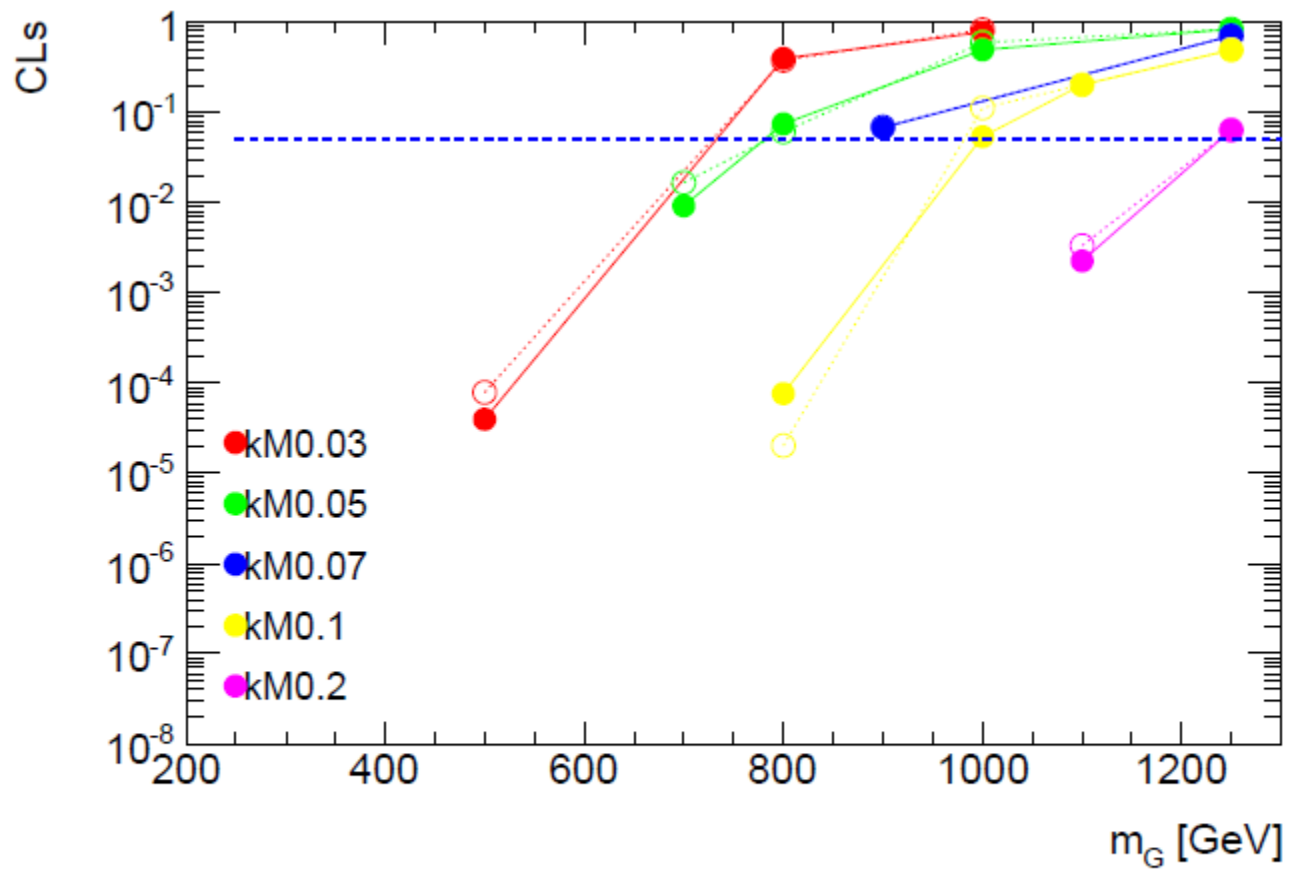


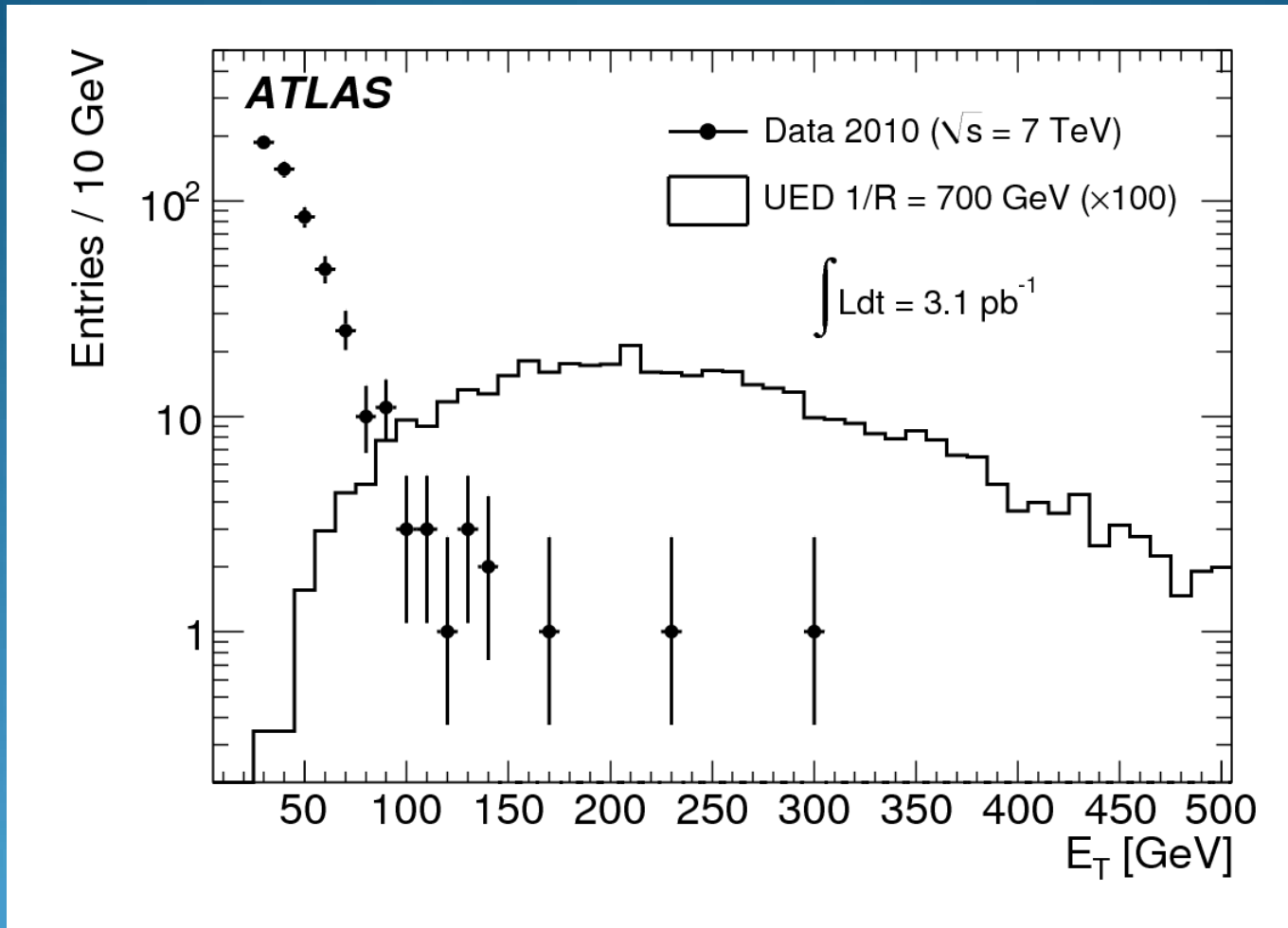
Figure 23: CLs expected (solid) and observed (open) values for various Graviton signals of different  $k/\overline{M}_{Pl}$  represented by a different color. The dashed horizontal line represents the 95% CL for exclusion.

Essentially, for a given mass, the cross-section varies  $\sim(k/M)^2$ .

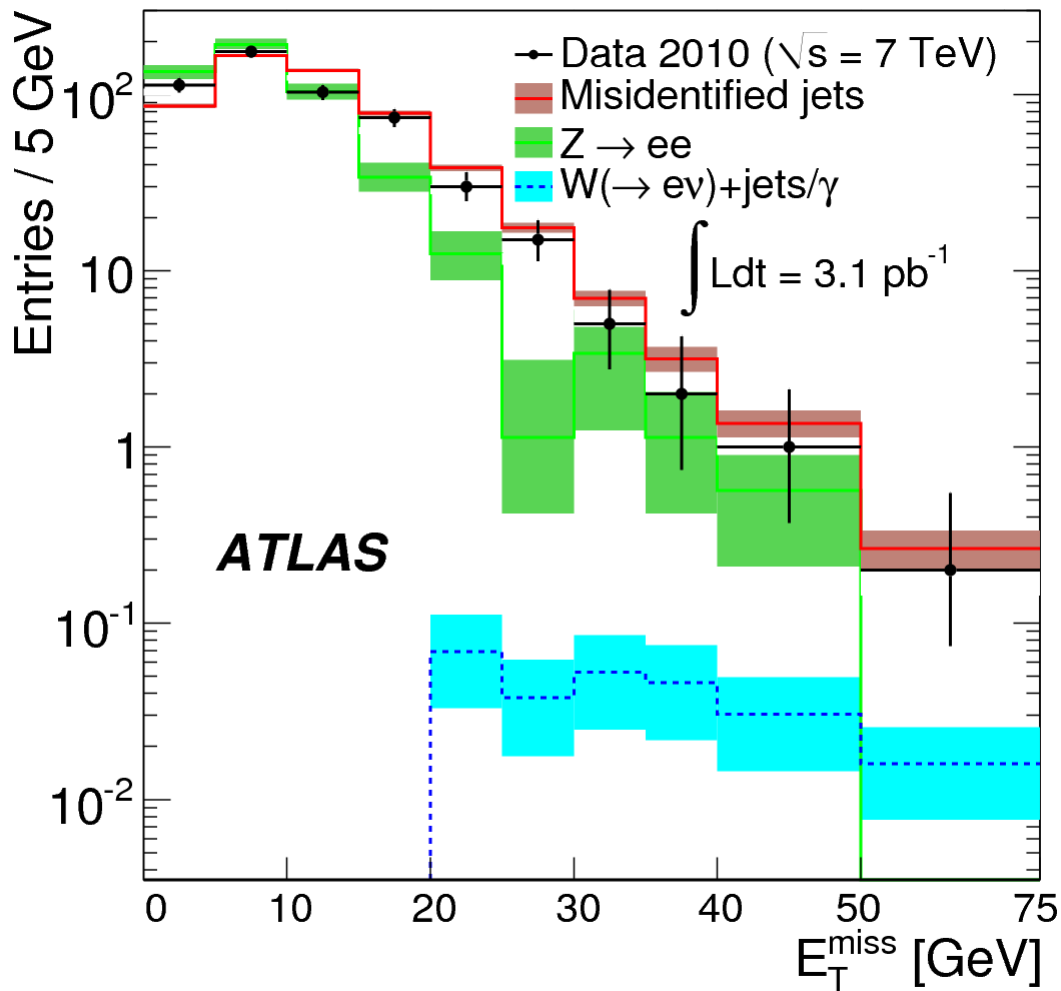
What we did here is compute the limit for a given value of  $k/M$  ( $\mu=1$ , mass fix) and then find the 95% CL by re-scaling the cross-section with  $\mu$ .

Afterwards,

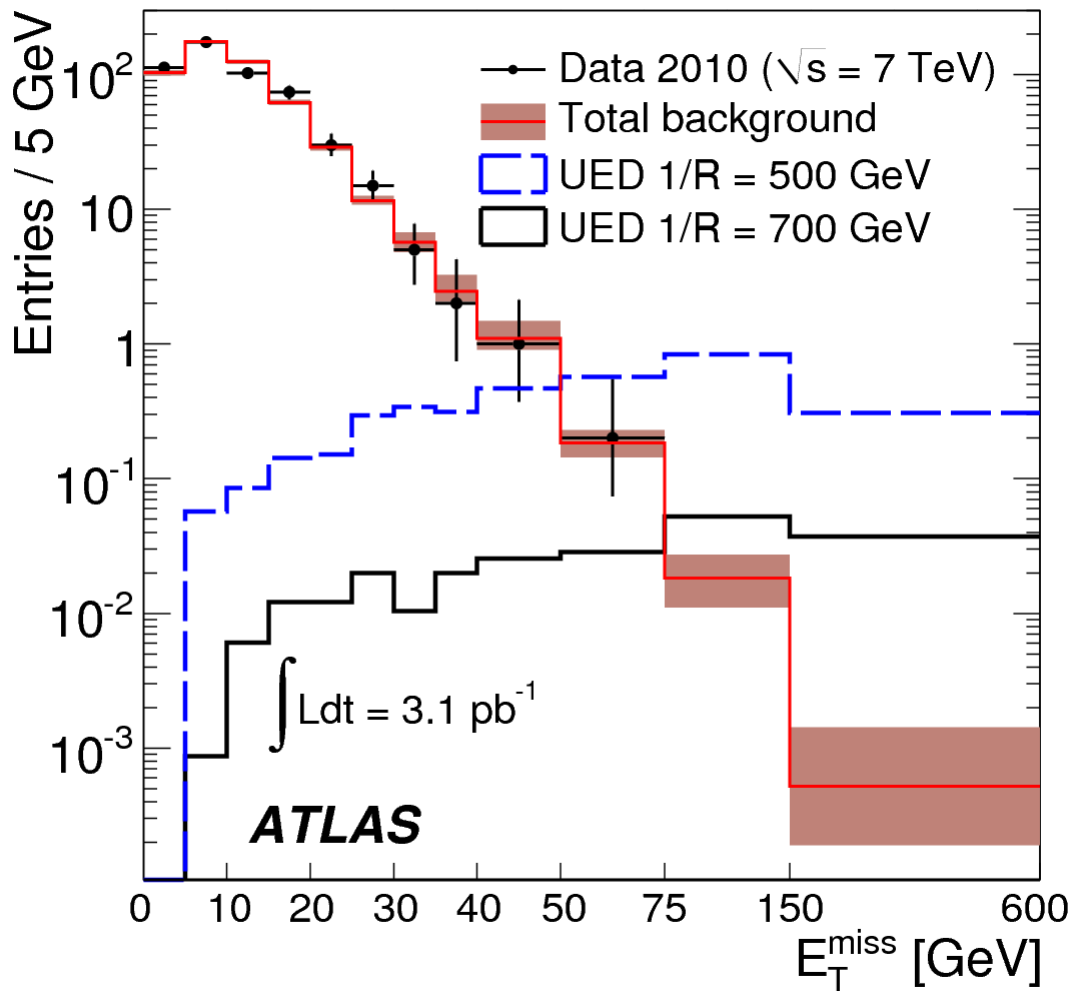
the associated value of  $k/M$  for the final value of  $\mu$  is obtained and quoted as the limit.



$E_T$  spectrum of the leading photon for the  $\gamma\gamma$  candidate sample and for UED  $1/R=700$  GeV MC events (normalized to 100 times the leading order (LO) cross section).



$E_T^{\text{miss}}$  spectra for the  $\gamma\gamma$  candidates,  
 for the  $Z \rightarrow ee$  and misidentified jet samples used to model the QCD background  
 (each normalized to the number of  $\gamma\gamma$  candidates with  $E_T^{\text{miss}} < 20 \text{ GeV}$ ),  
 and for the  $W \rightarrow ev + \text{jets}/\gamma$  background (normalized to its expected total of  $\sim 0.4$  events).  
 Variable sized bins are used, and the vertical error bars and shaded bands show the statistical errors.



$E_{\text{miss}}^{\text{T}}$  spectra for the  $\gamma\gamma$  candidates, compared to the total SM background as estimated from data.

Also shown are the expected UED signals for  $1/R=500 \text{ GeV}$  and  $700 \text{ GeV}$ .

Variable sized bins are used, and the vertical error bars and shaded bands show the statistical errors.

$E_T^{miss}$ [GeV]	Data	Predicted Background Events				Expected Signal Events	
	Obs.	Total	Z	anti-isEM	W	1/R=700 GeV	750 GeV
0-20	465	$465.0 \pm 9.1$	$167.9 \pm 8.3$	$297.1 \pm 3.7$	$0.0 \pm 0.0$	$0.02 \pm 0.0$	$0.01 \pm 0.0$
20-30	45	$40.5 \pm 2.2$	$4.9 \pm 1.8$	$35.5 \pm 1.3$	$0.1 \pm 0.1$	$0.03 \pm 0.01$	$0.01 \pm 0.0$
30-50	9	$10.4 \pm 1.3$	$2.0 \pm 1.2$	$8.2 \pm 0.6$	$0.2 \pm 0.1$	$0.08 \pm 0.01$	$0.06 \pm 0.01$
50-75	1	$0.92 \pm 0.23$	$0.00 \pm 0.00$	$0.84 \pm 0.22$	$0.08 \pm 0.05$	$0.14 \pm 0.01$	$0.10 \pm 0.01$
75+	0	$0.32 \pm 0.16$	$0.00 \pm 0.00$	$0.28 \pm 0.16$	$0.04 \pm 0.03$	$4.21 \pm 0.06$	$2.49 \pm 0.04$

Table 6: For various  $E_T^{miss}$  ranges, the number of observed data events as well as the predicted SM backgrounds (estimated from data) and expected signal for 1/R values of 700 and 750 GeV. The errors listed are statistical only. The first row, for  $E_T^{miss} < 20$  GeV, is the control region used to normalize the QCD background prediction to the number of observed  $\gamma\gamma$  events (events passing baseline + isolation + isEMloose cuts).

# Systematic uncertainties

## Photon reconstruction and identification efficiency

- Shower shape variables data/MC differences → 2%
- Extrapolation to higher ET → +2%
- Pileup → +1.6%
- Dead material simulation in detector geometry → +1.4%
- LAr gain cell bug in first data periods (300 nb<sup>-1</sup>) → +0.03%  
→ **3.5%**

## Photon isolation and ET data/MC differences

- Isolation 10% data/MC differences effects on signal acceptance → negligible
- ET 10% data/MC differences →  
1/R = 300 – 460 – 600 – 700 – 800 - 900 GeV  
4% - 2% - 1% - 1% - 0.7% - 0.5%

# Systematic uncertainties

## MET resolution data/MC differences

Data/MC 20 % difference in resolution affects signal acceptance

→ 0.2 % – 0.1 % for  $1/R = 300 - 900$  GeV

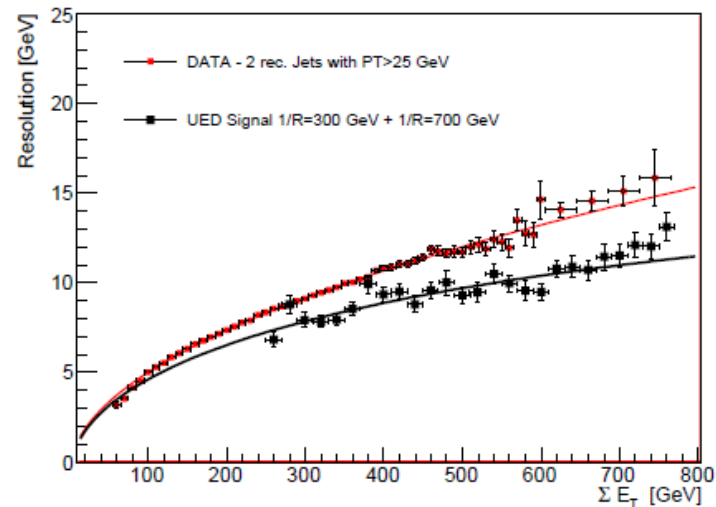
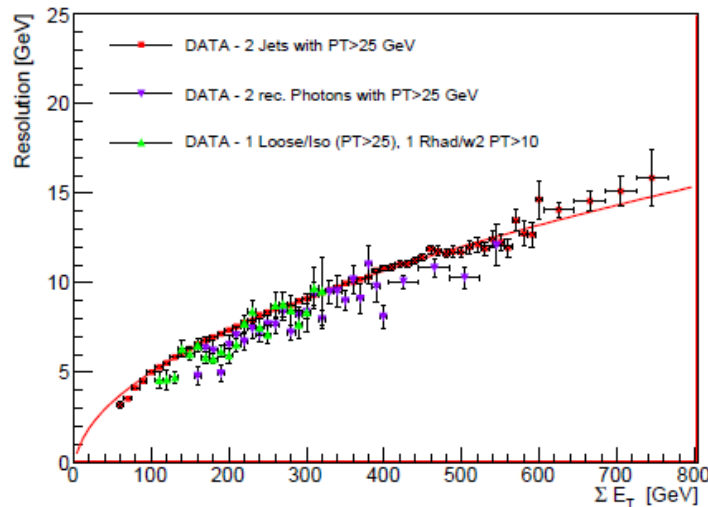


Figure 48:  $E_T^{miss}$  resolution curves as a function of  $\Sigma E_T$  for events passing trigger and cleaning cuts and containing 2 reconstructed jets with  $p_T > 25$  GeV and the same  $\eta$  cuts defined in this analysis (red) for events passing the baseline selection cuts (purple) and events in which the leading photon passes the isEMLoose and isolation cuts and has  $p_T > 25$  GeV, while the second leading photons has  $p_T > 10$  GeV and passes the Rhad and w2 photon identification cuts (green).



# Systematic uncertainties

## MET scale data/MC differences

Data/MC difference in scale affects signal acceptance

→ 3.7 % – 0.1 % for  $1/R = 300 - 900$  GeV

Topo-clusters matched to a truth photon from a KK photon decay labeled as EM clusters  
For these, scale uncertainty is 3% (see ref [32,33] of backup note)

All other topo-clusters are labeled as Hadronic clusters  
and are assigned a  $p_T$  and  $\eta$  dependent scale uncertainty  
(see ref [32,34,35] of backup note)  
motivated by data/MC differences in  $E/p$

## Pileup affects MET resolution

→ Negligible effect on signal acceptance

# Systematic uncertainties

## Parton distribution functions

For  $1/R=700(300)$  GeV

Compare cross-sections for following scenarios

MRST2007LOm (ATLAS MC09)

CTEQ66 (NLO) central value  $\rightarrow \Delta$  MRST-CTEQ  $\rightarrow +3\%$  (+7%)

CTEQ66 for its full set of errors  $\rightarrow \Delta$  CTEQcentral-CTEQ  $\rightarrow 6\%$  (4%)

Add both differences in quadrature

$\rightarrow 7\%$  (8%)

# Systematic uncertainties

## Data driven background estimation method

Zee fraction  $36 \pm 22$  % varied within its fit error

→ Predicted background  $\pm 0.10$

Remove the isolation cut

→ Predicted background + 0.37

Anti-loose control sample defined as events where both photons fail loose selection

→ Predicted background - 0.08

→  **$0.32 \pm 0.16$  (stat) + 0.37 / - 0.10 (syst)**

# Statistical interpretation <<features>>

## Bayesian <<features>>

- Non-integer estimated number of background events gives the same limit as zero events
- Background systematic uncertainties for zero events observed have no effect on the limit

## Frequentist <<features>>

- If one observes a small number of events (0,1,2,3), including the systematics will improve the limit!

## Feldman Cousins <<features>>

Properly interprets non-integer estimated number of background events but similar behavior as frequentist approach

Still being discussed

$\Lambda R =$	10	15	16	18	20	21	24	26	30
Cross section [pb]	3.41	2.99	2.95	2.88	2.73	2.72	2.60	2.56	2.43
Masses [GeV]									
$m(q^*)$	788	804	806	811	815	817	822	825	830
$m(l^*)$	715	718	718	719	719	720	721	721	722
$m(g^*)$	830	851	854	860	865	868	874	878	885
$m(\text{gamma}^*)$	700	700	700	700	700	700	700	700	700
$m(Z^*)$	734	739	740	741	743	743	745	746	748
$m(W^*)$	734	739	740	741	742	743	745	746	747

Table 9: Cross section and KK particle masses for different  $\Lambda R$  values for  $1/R=700\text{GeV}$ .

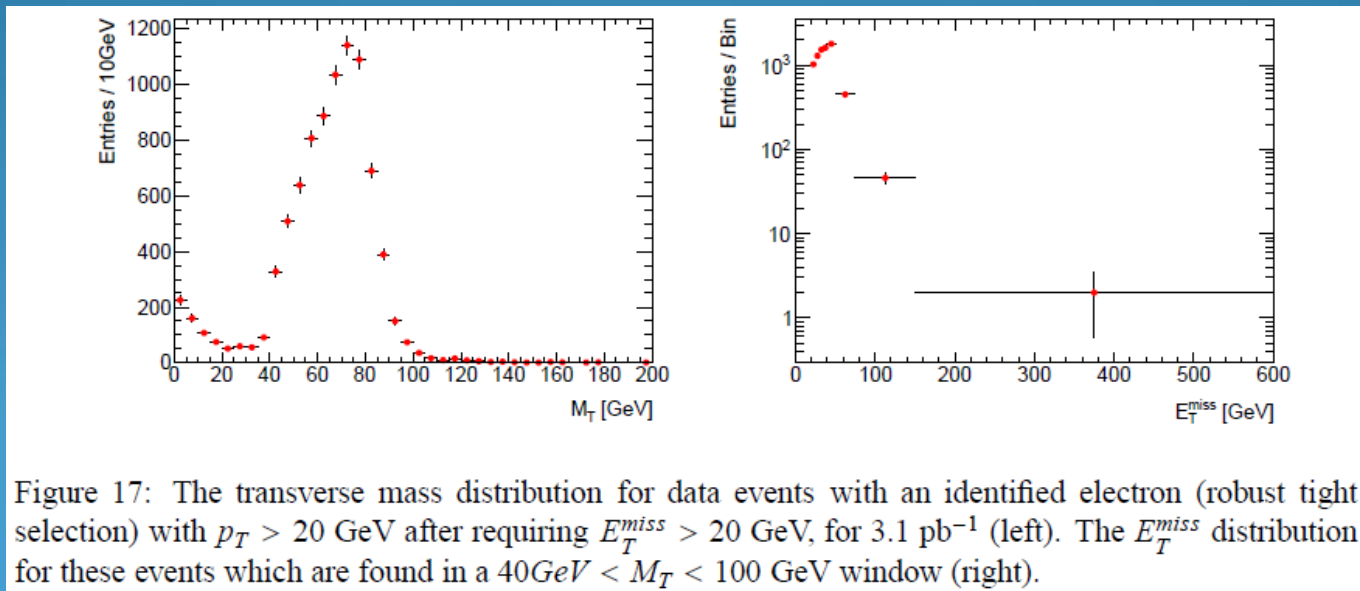
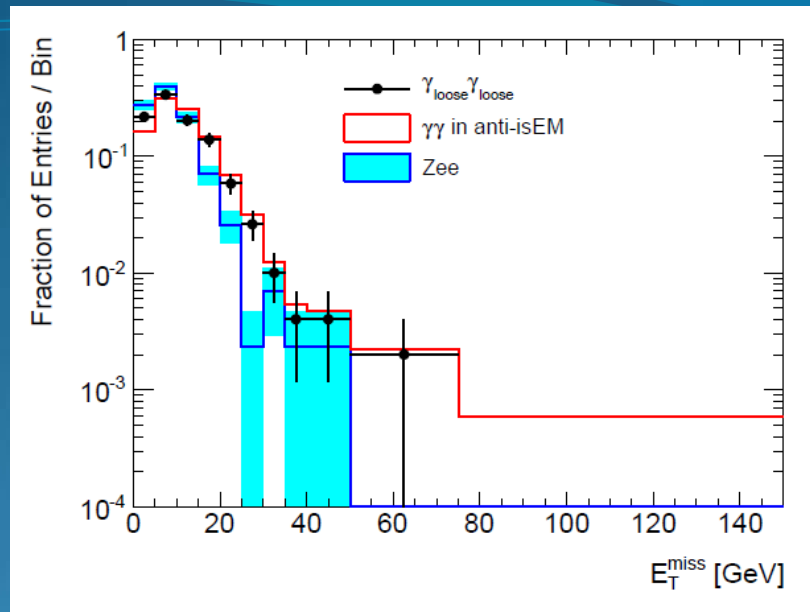


Figure 17: The transverse mass distribution for data events with an identified electron (robust tight selection) with  $p_T > 20$  GeV after requiring  $E_T^{miss} > 20$  GeV, for  $3.1 \text{ pb}^{-1}$  (left). The  $E_T^{miss}$  distribution for these events which are found in a  $40 \text{ GeV} < M_T < 100 \text{ GeV}$  window (right).

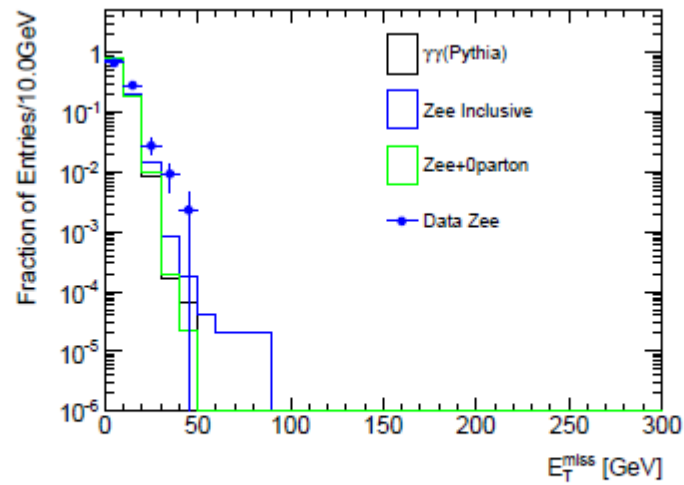


Figure 13:  $E_T^{miss}$  distributions from  $Z \rightarrow ee$  events in data and MC and  $\gamma\gamma$  MC events.

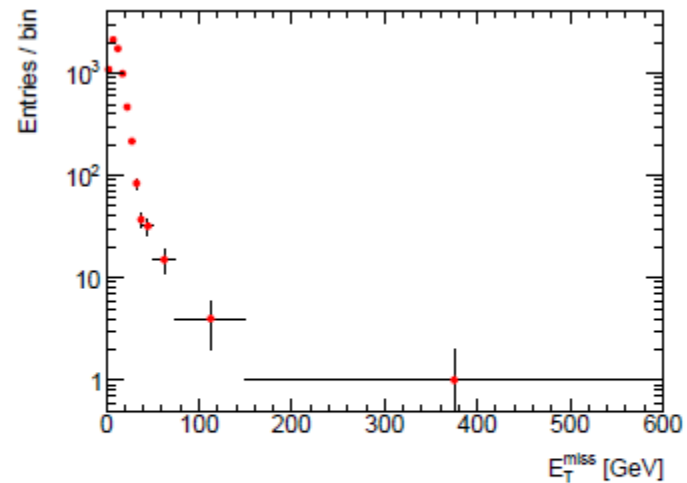
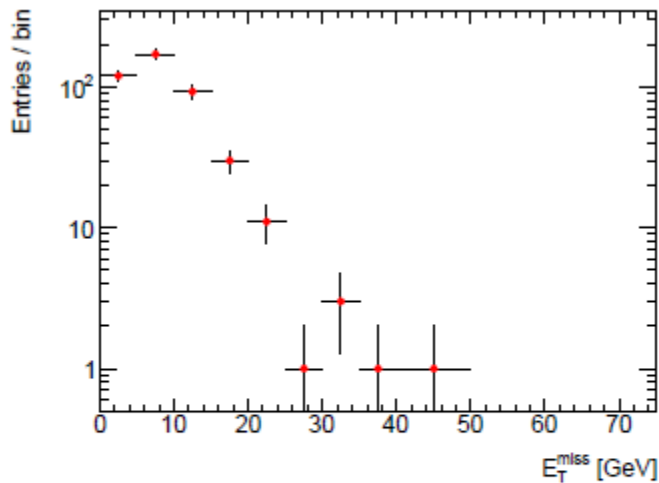
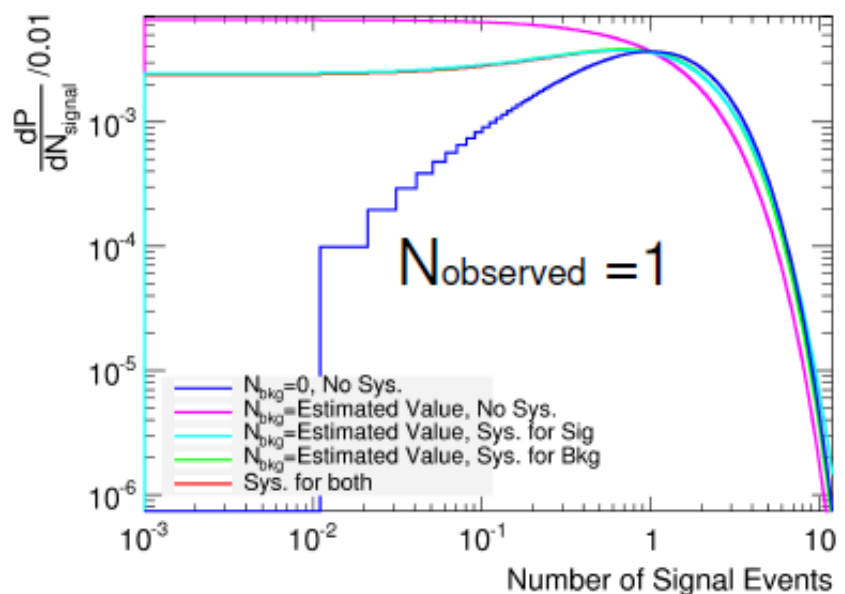
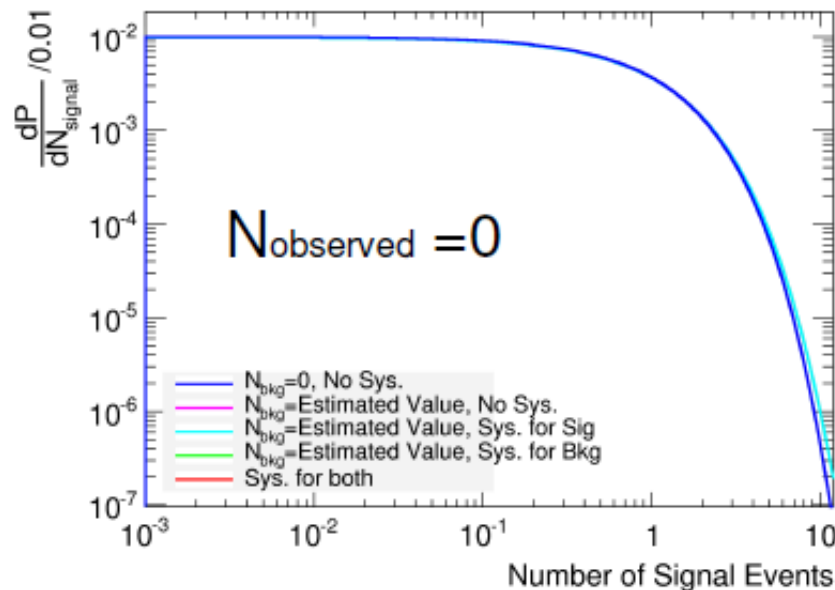


Figure 14:  $E_T^{miss}$  distribution for  $Z \rightarrow ee$  data events using  $3.1 \text{ pb}^{-1}$  (left).  $E_T^{miss}$  distribution for all data events ( $3.1 \text{ pb}^{-1}$ ) passing the baseline and photon isolation cuts, requiring that at least one of the most energetic photon candidates fail the isEMloose selection (right).

<b>1/R [GeV]</b>	<b>Gaussian</b>	<b>Log-Normal</b>	<b>Uniform</b>	<b>D0</b>	<b>CDF</b>
300	3.13	3.09	3.03	3.13	3.14
460	3.13	3.09	3.03	3.13	3.14
600	3.12	3.08	3.03	3.11	3.12
700	3.12	3.08	3.03	3.11	3.12
800	3.12	3.08	3.03	3.11	3.12

Table 8: Limits calculated with three different priors are shown. The limits vary slightly as  $1/R$  changes, since the systematics are not identical for various signal points. As a cross-check, limits obtained from two simple calculators developed by the D0 and CDF Collaborations are also included.





Limits from different configurations of systematics for Nobs =0 and 1.

Nb:Expected Bkg Events	0 obs. event	1 obs. event
Nb = 0, No systematics	2.99	4.74
Nb = 0.33, No systematics	2.99	3.81
Nb = 0.33, systematics for signal	3.14	4.70
Nb = 0.33, systematics for background	2.99	4.47
Nb = 0.33 systematics for both	3.14	4.71

Feature of Bayesian limit, when Nobs = 0, after integration bkg priori, the shape of probability density function is independent on background, and thus the limit is independent on background information.